Received: 12 May 2019 | Revised: 24 July 2019 | Accepted: 24 July 2019

DOI: 10.1002/aoc.5180

FULL PAPER

WILEY Applied Organometallic Chemistry

High Catalytic Performance of Mesoporous Dual Brønsted Acidic Ternary Poly (Ionic Liquids) for Friedel-Crafts Alkylation

Xiao Sha[1,2] | **Xiaoli Sheng**[1,2] | **Yuming Zhou**[1,2] | **Beibei Wang**[1,2] | **Yonghui Liu**[1,2] | **Jiehua Bao**[1,2]

[1]School of Chemistry and Chemical Engineering, Southeast University, Nanjing 211189, China

[2]Jiangsu Optoelectronic Functional Materials and Engineering Laboratory, Nanjing 211189, China

Correspondence
Xiaoli Sheng and Yuming Zhou, School of Chemistry and Chemical Engineering, Southeast University, Nanjing 211189, China; Jiangsu Optoelectronic Functional Materials and Engineering Laboratory, Nanjing 211189, China.
Email: xlsheng@seu.edu.cn; ymzhou@seu.edu.cn

Funding information
"Six Talents Pinnacle Program" of Jiangsu Province of China, Grant/Award Number: JNHB-006; Fund Project for Transformation of Scientific and Technological Achievements of Jiangsu Province of China, Grant/Award Number: BA2014100; Qing Lan Project of Jiangsu Province, Grant/Award Number: 1107040167; Innovative Research Group Project of the National Natural Science Foundation of China., Grant/Award Numbers: 21376051, 51673040, 21306023 and 21676056

A newfangled cross-linked dual Brønsted acidic ternary mesoporous poly (ionic liquids)(MPILs) with mesoporous structure was successfully synthesized with divinylbenzene as cross linker, 1-vinyl-3-butyl imidazole bromide and sodium p-styrene sulfonate as functional group through an ordinary post-modification method and anion exchange process. A sponge-like mesoporous tunnel structure was observed and the obtained P (BVS-SO_3H)-SO_3CF_3 sample appeared a relatively high thermal stability, a large surface area (up to 286.8 m^2/g) and great pore volume (0.73 cm^3/g). The abundant dual acidic group of sulfonic acid and trifluoromethanesulfonic acid of the composite in the polymer framework impart Brønsted acidity. For the sake of demonstrating our claims, the sample has been used as a novel solid acid catalyst for the reaction of alkylation of o-xylene with styrene to 1-diphenylethane (PXE). Under optimal reaction conditions (reaction under 120 °C for 3 hr, catalyst amount was 0.5 wt% of the reaction system, and the mass ratio of o-xylene/styrene was 7.5:1, a 100% conversion of styrene and 93.7% PXE yield was acquired. After four times recycle, the yield remains 53.3%. Comparing with the commercial liquid acid catalyst, it processing a higher catalytic property and recyclability. Moreover, this fresh dual acidic heterogeneous catalyst owning a promising future applied in other acidic catalytic reactions and provide a new method to modify catalyst.

KEYWORDS
dual-acid catalysis, functional, mesoporous structure, polymers

1 | INTRODUCTION

The alkylation of *o*-xylene with styrene is a significant industrial Friedel-Crafts reaction, the research has last for a very long time for the product phenylxylylethane (PXE) exhibits a great range of application, such as the pressure-sensitive record materials, a heating medium, an electric-insulating oil and other applied materials.[1–3] Typically, Brønsted acidic, such as H_2SO_4, HCl and HF are usually used as the catalyst of the reaction[4]. However, these traditional catalysts are difficult to separate and always show a low active performance, which make them high-cost catalysts. In order to overcome these drawbacks, it is significant and urgent to discover an environment-friendly heterogeneous solid catalysts for this Friedel-Crafts reaction.

Increasing attention has recently been drawn to ionic liquids (ILs) because of its broad applicability, from solvent to catalysis chemistry with the properties of unique combination ability, low flammability, negligible vapor pressure, controllable acidity and basicity, high ionic conductivity and so on.[5] One important utilization of ILs is that they display wide applications as a catalyst in many organic reactions. However, the liquid state of ionic liquids limits their recyclability which may attribute to the drastic loss in catalytic activity. Meanwhile, the low surface area of current homogeneous catalyst of ionic liquids catalysts limits their catalytic efficiency and is more difficult to separate from the reaction system than heterogeneous ones, which leading to their low competitiveness in industrial applications. Synthesis of a heterogeneous catalyst with porous structure would be a short-cut way to obtain better catalytic efficiency and recycling performance than current ionic liquids catalysts.

As heterogeneous catalyst, solid acidic catalyst has been widely used in esterification[6], hydrogenation reaction[7], Beckmann rearrangements[8], Friedel-Crafts acylation reaction. Mesopores poly (ionic liquids)(MPILs), as a special type of ionic liquids (ILs),is composed of ILs containing polymerizable units, crosslinkers and other functional groups with mesoporous structure[9,10]. Thus, MPILs show some unique properties which not only combined that of ILs and polymer materials, but also allowed for the existence of fresh properties for a wide range of applications in separations, catalysis and electricity[4,11–15]. The preferences of MPILs compared to the corresponding homogeneous ILs are inspired by the superiorities of easy separation and controllable structure[16]. Theoretically, the exchange of intrinsic anions in MPILs by functional ones can bring some novel performances and constitute porous structure[3,11,17–24]. For example, Suo[25] has prepared a family of new mesoporous MPILs containing long chain carboxylate ILs as anion functional group through a methodology to create mesopores structure via microphase separation. In our previous work, we have successfully synthesized alkoxysilyl-functionalized polymer ionic liquid by solvothermal and post-synthesis method where ILs act as both template and silica source[26]. All these reports can strongly demonstrate the theory that the type of anion in MPILs can greatly influence their functionality and performance.

In this work, a newfangled dual Brønsted acidic MPILs has been reported via a facile post-modification method, in which ILs and sulfonic functional monomers were copolymerized by DVB as cross-linker, sodium p-styrenesulfonate as a functionl group and then -SO_3CF_3 group can be anchored into polymer chains by anion exchange. The -SO_3CF_3 and -SO_3H groups within the samples can significantly increase the effective acidic activity of the catalyst which is attribute to the performance of the target reaction of alkylation of o-xylene with styrene. Furthermore, a series of comparative experiments were put into effect to investigate the effect of different molar ratio of p-styrenesulfonate, and the amount of catalysts, the reaction condition of temperature and recycle times on the alkylation of o-xylene with styrene. The results of this paper may provide a promising insight in to the acidic reaction field.

2 | EXPERIMENTAL

2.1 | Materials

All chemicals and solvents were commercially available and used without any purification. 1-butyl-3-vinylimidazolium bromide (99 wt%) (B), 1,4-diethenylbenzen(80 wt%)(V), 2,2′-azobis (2-methylpropionitrile) (AIBN) were purchased from Aladdin Industrial Corporation, anhydrous ether (AR), sodium p-styrenesulfonate(-S), 1,4-epoxy-butan (AR) and ethanol absolute (AR) were purchased from Sinopharm Chemical Reagent Co., Ltd. o-xylene, styrene and tetrahydrofuran (THF) were supplied by Shanghai Lingfeng Chemical Reagent Co., Ltd.

2.2 | Preparation of catalysts

2.2.1 | Preparation of mesoporous P (BVS-SO_3Na)

As a typical run for compound of P (BVS-SO_3Na), 2.44 g (15 mmol) of 1,4-divinyl-benzene (D) was added into a solution containing 4.0 ml of deionized water followed by addition of 20 ml of THF, then add the appropriate x amount of sodium p-styrene sulfonate (x = 1.5, 2.0, 2.5, where x represents the molar ratio of sodium p-styrene sulfonate/1-vinyl-3-butyl imidazole bromide/DVB at x/1.0/2.0.) was introduced in a 100 ml Schlenk flask. After stirring at ambient temperature for 2 hr, 0.16 g 2, 2′-azobis (2-methylpropionitrile) (AIBN) was added into the above mixture and continue stirring under ambient temperature for 3 hr. Then, the mixture was deoxygenated for 30 min and backfilled with N_2 continually, followed by vigorous magnetic stirring at 80 °C for 18 hr. After evaporation of the solvents at room temperature, the P (BVS-SO_3Na) sample was washed with a large amount of EtOH before centrifugal separation, and dried under vacuum at 343 K for 24 hr. Then, the resultant yellow powder was ground for further applications.

2.2.2 | Preparation of mesoporous P (BVS-SO_3H)

To get a P (BVS-SO_3H) sample, the P (BVS-SO_3Na) sample was further ion-exchanged by using 2 M sulfuric acid. As a typical route, 1.5 g of P (BVS-SO_3 Na) was dispersed into 15 ml anhydrous ethanol solution, then 15 ml of 2 M H_2SO_4 was added with vigorous magnetic stirring by constant pressure funnel. After stirring for 24 hr under ambient temperature, the sample was treated by centrifugation and washed with ethyl ether until the supernatant was neutral and repeat this step for three times. Then, dried the sample under high vacuum at 343 K for 24 hr, finally P (BVS-SO_3H) was obtained.

2.2.3 | Preparation of mesoporous P (BVS-SO_3H)-SO_3CF_3

Firstly, 1.0 g of P (BVS-SO_3Na) was added to the solution with 25 mL of toluene and 3 ml HSO_3CF_3 and string for 24 hr at ambient temperature and filter to remove the solvent. Then, wash the sample with anhydrous ether solution and dry at 333 K for 6 hr. After that, repeat this operation once again, the P (BVS-SO_3H)-SO_3CF_3 sample was obtained finally.

2.3 | Characterization of catalysts

The construction and morphology of the catalysts were examined through Fourier transform infrared (FT-IR, FTIR-6700), scanning electron microscopy (SEM, FEI Inspect F50) and transmission electron microscopy (TEM, JEOL, JEM-2100). The N_2 adsorption/desorption isotherms were recorded on an ASAP 2020 apparatus (Micromertics USA). And the specific surface area and pore size distributions were performed using Brunauer–Emmett–Teller (BET) and Barrett–Joyner–Halenda (BJH) model, respectively. ~~a~~ A Rigaku ThermoPlus TG8120 system was used under a rate of 10 °C min^{-1} in air to excute Thermo Gravimetric Analysis (TGA).

2.4 | Determination of alkylation catalyst activity

The alkylation of o-xylene and styrene was used to evaluate the catalytic performance of the prepared products. Through a typical procedure, 30 g o-xylene, 4 g styrene, and catalyst (x wt%, where x represents relative to the weight of the whole reaction system) were blended in a 250 ml flask. Then, we heated the mixture to 120 °C in an oil bath with continued magnetic stirring for 3 hr under common pressure. And after the procedure, catalyst sample was recycled through vacuum filter procedure and dry at 60 °C for 12 hr. The catalyst performance of the samples were detected by gas chromatograph, GC 9890A.

3 | RESULT AND DISCUSSION

3.1 | Catalysts characterization

It can be observed in the Figure 1 A that the different molar ratio of sodium p-styrene sulfonate of the P (BVS-SO_3Na) never influence the peaks in the FT-IR spectra. Peaks at 2970 and 2920 cm^{-1} are associated with the C–H stretching of C–H bending of CH_3 and CH_2 functional group respectively. Peaks at 1449, 789 and 722 cm^{-1} are associated with in-plane and out-of-plane rings of C–H bending within CH_3 and CH_2 functional group The bands at around 1633 and 1224 cm^{-1} is a to the are derived from C=N and C–N stretching for imidazole. Peaks at 1157and 1041 cm^{-1} represents the asymmetric and symmetric stretching of the O=S=O bonds within sulfonic groups[27,28]. In Figure 1 B, the new bands at around

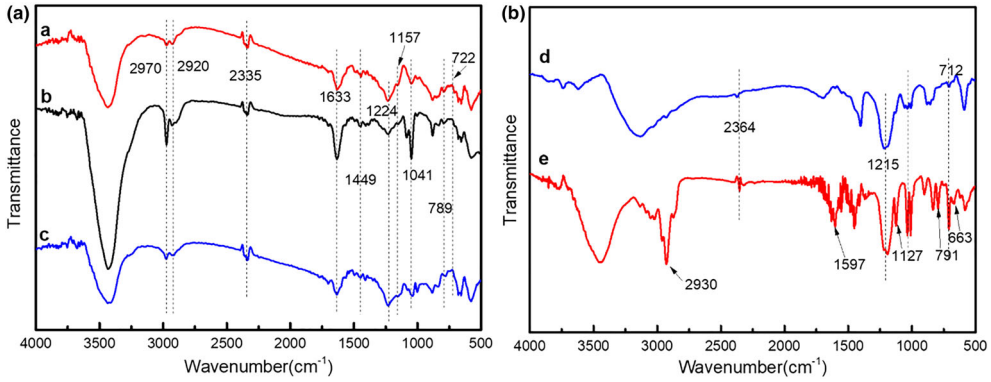

FIGURE 1 A: FT-IR spectra of different ratio of P (BVS- SO3Na), a) x = 1.5, b) x = 2, c) x = 2.5; B: FT-IR spectra of d) P (BVS-SO3H) and e) P (BVS-SO3H)-SO3CF3

1597, 1127, 791, 663 cm^{-1} is associated with the existence of S-O and C-F in -SO_3CF_3 functional group respectively. And the peak of benzene ring in P (BVS-SO_3H) is red-shift, which indicate the much more stable combination of the group. While the peaks at 2335 cm^{-1} in Figure 1 A and peak of benzene ring at 2364 cm^{-1} in Figure 1 B is commonly attribute to the CO_2 in the atmosphere. All the above results indicate the oxidation and the successful introduction of -SO_3CF_3 groups onto the PILs through the anion exchange route.

As demonstrated in Figure 2, the P (BVS-SO_3Na) and P (BVS-SO_3H)-SO_3CF_3 sample exhibit a type-IV curve with a diminutive hysteresis loop of type H1 in the relative pressure (P/P0) region of 0.5–1.0, which can indicate the existence of mesopores within the samples. Accordingly, the pore size of P (BVS-SO_3Na) is mainly distributed at 20 nm and that of P (BVS-SO_3H)-SO_3CF_3 was distributed at around 35 nm. The BET data were listed in the Table 1. And the BET surface of P (BVS-SO_3Na) and P (BVS-SO_3H)-SO_3CF_3 are 417.5cm^2/g and 286.9cm^2/g, respectively. The smaller surface area of P (BVS-SO_3H)-SO_3CF_3 is attributed to the partial blockage and destruction of the mesopores by acid in anion exchange. While the P (BVS-SO_3H) sample shows a surprisingly low BET surface of 17.89cm^2/g and there is almost no mesopores pore in the P (BVS-SO_3H).

As we can observe in the Figure 3, P (BVS-SO_3Na) and P (BVS-SO_3H)-SO_3CF_3 show an analogous sponge-like porous structure with a large amount of mesoporous architecture within the samples which could thanks to the solvent extraction procedure which manufacture a plethora of mesopores within the sample. The crosslinking of the monomers and the solvent extravagation procedure construct the mesoporous structure. Nevertheless, the P (BVS-SO_3Na) exhibits a more solid construction than P (BVS-SO_3H)-SO_3CF_3 which may as a result of the process of ion exchange of $CF_3SO_3^-$. In picture (b), it can be easily observed that the porous structure is blocked and is different from the

TABLE 1 The Textural Parameters of Various Polymer Acid Catalysts

MPILs	S_{BET}[a] (m^2 g^{-1})	D_{AV}[b] (nm)	V_p[c] (cm^3 g^{-1})
P (BVS-SO_3Na)	417.50	9.61	0.81
P (BVS-SO_3H)	17.89	25.04	0.05
P (BVS-SO_3H)-SO_3CF_3	286.90	11.79	0.73

sponge-like structure which may due to the introduction of H_2SO_4 through the acidification step, the structure of which choke the mesoporous texture. But the framework of cross-linked dual Brønsted acidic MPILs kept tight during the whole anion exchange process and the loose porous structure of it is consistent with the BET analysis result.

It can be obviously observed in Figure 3(d), (e) and (f) that P (BVS-SO_3Na) exhibits an abundant hierarchical net-like mesoporous construction and the TEM of P (BVS-SO_3H)-SO_3CF_3 shows a different conformation, which can be owing to the re-crosslinking and partly breakage during the introduction of CF_3SO_3H. While the TEM of P (BVS-SO_3H) shows a relatively tight structure, which is correspond to the SEM result that the pores within the framework is blocked.

Since two different kinds of strong Brønsted acids were utilized to decorate the catalyst through the impregnation step with P (BVS-SO_3Na) powders, it was of great necessity to verify the thermal and structural stability of the product after acidic treating. TG curves of the three samples were presented in Figure 4. All the synthesized products comprise three main weight loss steps at 50–120 °C, 260–395 °C and 410–600 °C[27,29–31]. When the temperature is lower than 120 °C, the first stage of the curve, it could be observed that P (BVS-SO_3Na) and P (BVS-SO_3H)-SO_3CF_3 show a consistent thermogravimetric loss at about 8.7% which may due to the combined water within the samples. While the weight loss of P (BVS-SO_3H) is nearly double of that of the other two samples

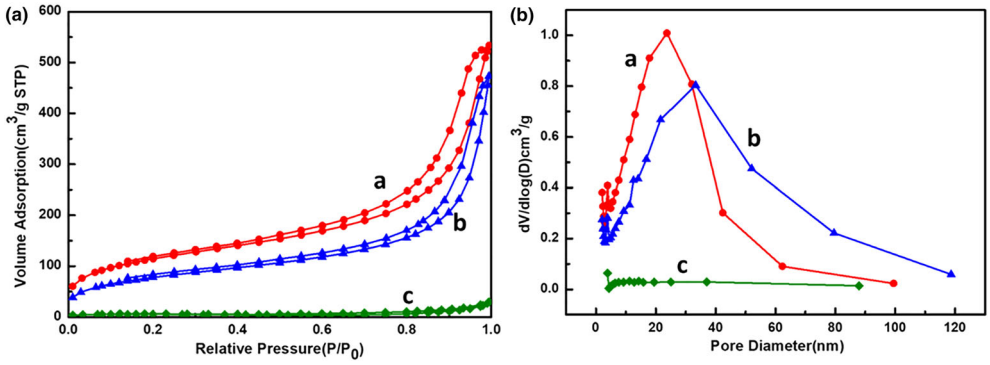

FIGURE 2 A: N2 adsorption–desorption isotherm and B:Pore size distribution of a) P (BVS-SO3Na), b) P (BVSSO3H)-SO3CF3, c) P (BVS-SO3H)

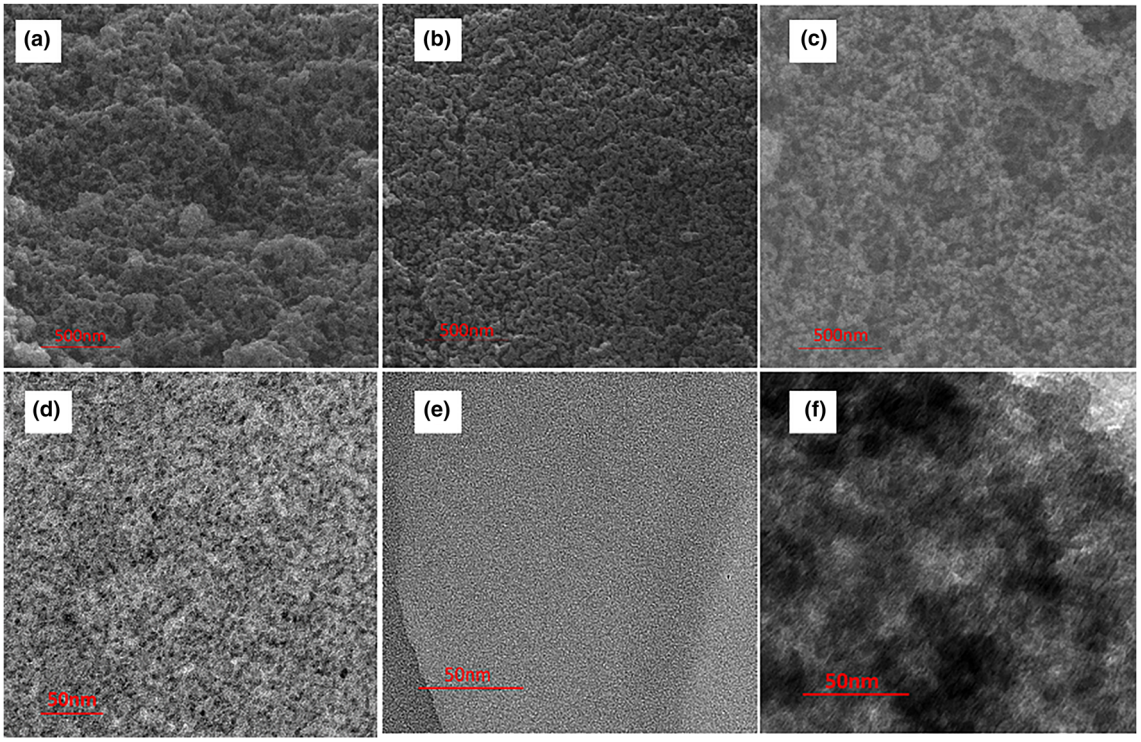

FIGURE 3 SEM image of a) P (BVS-SO3Na), b)P (BVS-SO3H) and c) P (BVS-SO3H)-SO3CF3; TEM image of d) P (BVS-SO3Na), e)P (BVS-SO3H) and f) P (BVS-SO3H)-SO3CF3

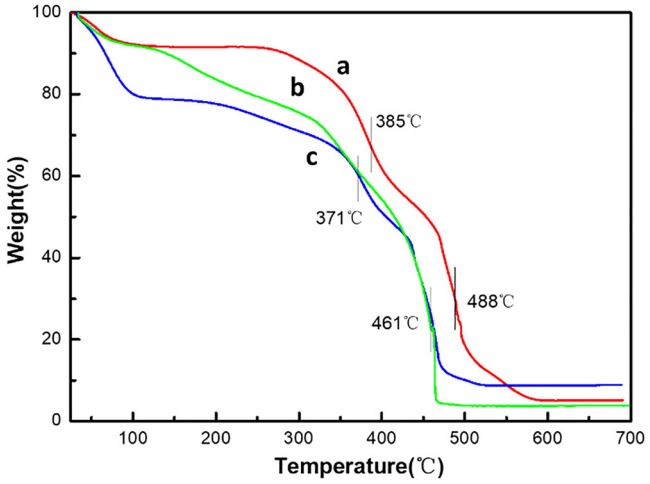

FIGURE 4 TG curves of a) P (BVS-SO3Na), b) P (BVS-SO3H) and c) P (BVS-SO3H)-SO3CF3

which reflected that the hydrophilic property of P (BVS-SO_3H) is much better ascribed to the acidification step of sulfuric acid. The disintegration of acidic groups is corresponding to the second stage, P (BVS-SO_3Na) shows a minor advantage of thermal stability than P (BVS-SO_3H) and P (BVS-SO_3H)-SO_3CF_3[29,32,33]. Apparently, the catalyst is stable enough before 300 °C. The last stage is attributed to the collapse of the frameworks, P (BVS-SO_3H) and P (BVS-SO_3H)-SO_3CF_3 only have about less than 5% of residue left, while the residue of P (BVS-SO_3H) is twice as much as that of other two samples. Considering the SEM and TEM analysis, the H_2SO_4 may leave in the remains. Obviously, the P (BVS-SO_3H)-SO_3CF_3 is slightly less stable than P (BVS-SO_3Na) and the remains of P (BVS-SO_3Na) is sort of more than that of P (BVS-SO_3H)-SO_3CF_3 which may all attribute to the small partly destruction of precursor by introducing acidic -SO_3CF_3 groups during anion exchange.

3.2 | Catalytic performance evaluation

3.2.1 | Catalysis performance of P (BVS-SO_3H)

Effect of the catalyst amount

In this section, the catalysts with different ratio of sodium p-styrenesulfonate are investigated through the target alkylation of o-xylene with styrene (showed in Figure 5). The specific reaction process is listed in the experimental section. It can be observed that when the x = 2 the catalyst perform a much better yield (showed in Table 2). Too little or too much sodium p-styrenesulfonate both effect the property of the sample and the reason of this phenomenon may attribute to the polymerization of different functional groups during the process which may block the active site of the catalyst. Then we choose the sample with the system of sodium

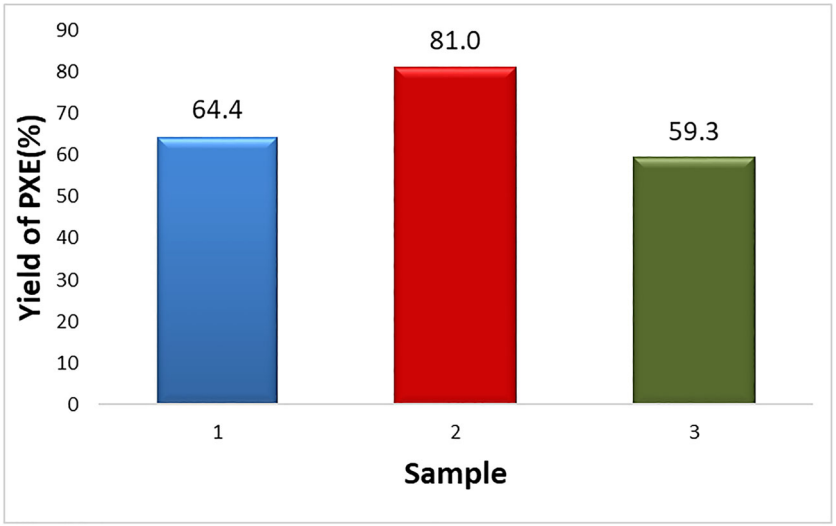

FIGURE 5 The catalysis performance of catalyst different x ratio of sodium p-styrenesulfonate in P (BVS-SO3H): a) x = 1.5, b) x = 2, c) x = 2.5

TABLE 2 Yield of PXE and conversion of styrene with different x ratio of sodium p-styrenesulfonate in P (BVS-SO_3H)

Catalyst	Styrene conversion rate (%)	PXE yield (%)
P (BVS-SO_3H) (x = 1.5)	69.4	64.4
P (BVS-SO_3H) (x = 2.0)	90.1	80.0
P (BVS-SO_3H) (x = 2.5)	68.7	59.3

The reaction temperature is 120 °C and the addition is 0.5 wt%

p-styrene sulfonate/1-vinyl-3-butyl imidazole bromide/DVB/THF/H_2O at a molar ratio of 2.0/1.0/2.0/32.2/14.46 to carry out the following performance testing.

3.2.2 | Catalysis performance of P (BVS-SO_3H)-SO_3CF_3

Effect of the reaction temperature

Temperature of reaction was confirmed as another key factor of the catalysis performance. In order to optimize the reaction condition through a specific method, the catalysts addition was identical controlled under an amount of 0.5 wt%, and this section only changed the reaction temperature (40 °C, 60 °C, 80 °C, 100 °C, 120 °C, respectively) (showed in Table 3). Conversion rate (%) of styrene was another evidence to prove the catalyst performance. With the increasing of reaction temperature, the styrene conversion rate (%) gradually increased synchronously. The conversion rate (%) of styrene all reached 100% at the temperature of 120 °C. A relatively higher temperature condition will be better for the alkylation reaction of o-xylene and styrene, and under this temperature, styrene can achieve 100% which means that there is no styrene leave in the reaction system.

TABLE 3 Yield of PXE and conversion of styrene under different temperature

Catalyst	Temperature (°C)	Styrene conversion rate (%)	PXE yield (%)
P (BVS-SO_3H)-SO_3CF_3	40 °C	40.2	32.2
P (BVS-SO_3H)-SO_3CF_3	60 °C	51.0	44.8
P (BVS-SO_3H)-SO_3CF_3	80 °C	71.0	61.1
P (BVS-SO_3H)-SO_3CF_3	100 °C	83.1	73.3
P (BVS-SO_3H)-SO_3CF_3	120 °C	100.0	93.7

The addition is all the 0.5 wt%.

Effect of P (BVS-SO_3H)-SO_3CF_3 amount

The adequate reaction temperature has been confirmed to be 120 °C in the above section, in order to carry out further and more in-depth research, the aspect of addition amount of catalyst P (BVS-SO_3H)-SO_3CF_3 has been discussed to study its impact on the yield(%) of PXE (showed in Table 4). It is no doubt that with the augment of catalyst, it made a great influence on the PXE yield (%) for it can introduce more active sites which can be beneficial to provide more exposure of acidic sites. It is easy to explain that the more active site we introduce, the stronger the catalyst will show in the reaction under the same reaction condition. Comparing with diverse addition amount of cross-linked mesoporous dual Brønsted acidic poly (ionic liquids) P (BVS-SO_3H)-SO_3CF_3, it can be easily observed that the yield of PXE almost achieve 100% with the catalyst is 0.5 wt%. When the addition of catalyst is under a relatively lower condition the catalysis performance is not good enough, while the increasing amount of catalyst never continually increase the yield of PXE.

TABLE 4 Yield of PXE and conversion of styrene under different amount of P (BVS-SO_3H)-SO_3CF_3

Catalyst	Addition (wt%)	Styrene conversion rate (%)	PXE yield (%)
P (BVS-SO_3H)-SO_3CF_3	0.075	100.0	39.5
P (BVS-SO_3H)-SO_3CF_3	0.250	100.0	77.8
P (BVS-SO_3H)-SO_3CF_3	0.500	100.0	93.7
P (BVS-SO_3H)-SO_3CF_3	0.600	100.0	89.3

The reaction temperature is all the 120 °C.

3.2.3 | Recyclability of P (BVS-SO_3H)-SO_3CF_3 and P (BVS-SO_3H) catalyst

Depending on the above research, the recyclability of P (BVS-SO_3H)-SO_3CF_3 and P (BVS-SO_3H) catalyst was investigated under the conditions of 120 °C and the amount of catalyst is 0.5 wt% (relative to the weight of the whole reaction system) is the optimal conditions. Though the catalyst showed great catalysis performance in the target alkylation, the recycling possibility of catalyst would be an effective way to estimate the performance of catalysts. In this section, we consider the styrene conversion rate (%) and PXE yield(%) to estimate the catalysis performance of the product and the reaction cycle is also used to evaluate the stability of it. It is remarkable that the recyclability of the catalyst we syntheses was not as stable as we anticipated. After the first catalyst reaction, the P (BVS-SO_3H)-SO_3CF_3 sample exhibits a gradually degradation of catalysis performance while the P (BVS-SO_3H) product display a sharp drop in Figure 6. It can also be observed through the Figure 6 that the property of P (BVS-SO_3H)-SO_3CF_3 is much better than that of P (BVS-SO_3H) through the reaction cycle test, the yield of PXE from 93.7% to 53.3% after 5 times repeating comparing to the yield from 81.0% to 40.6% after 5 times recycling. The possible reason is that the sulfonic acid groups within the structure of catalyst were destroyed after reaction of alkylation of o-xylene and styrene for high reaction temperature and some of acidic group -SO_3CF_3 may remain in the solvent of reaction system. All these may be the ground for the low recycling utilization. The SEM comparison of the two catalysts has been listed in supporting information.

The results of BET, SEM, TEM and TG analysis are corresponding to the result of catalysis performance of the P (BVS-SO_3H) and P (BVS-SO_3H)-SO_3CF_3. The blockage of the pores within the sample may result from the introduction of H_2SO_4 procedure in which the mesopores are stifled which can also explain the SEM and TEM result that the structure of P (BVS-SO_3H) is not the sponge-like one as the same of P (BVS-SO_3H) and P (BVS-SO_3H)-SO_3CF_3. All the above possible reasons lead to the catalysis property of P (BVS-SO_3H) is much weaker.

3.3 | Plausible mechanism of the catalyst

Figure 7 displays the possible construction mechanism of P (BVS-SO_3H)-SO_3CF_3. It is well known that HSO_3CF_3[34–38] as a kind of protonic super organic acid, whose acidity is much higher in organic solvent than common acid such as H_2SO_4. And the triflate is stable enough that the redox reaction cannot happen. In addition, entirely stability of network structure was greatly enhanced by the energy between covalent bond and the interaction between cations and anions. The copolymerization procedure consists of three main synthesis steps. Firstly, DVB, 1-vinyl-3-butyl imidazole bromide and sodium p-styrene sulfonate was crosslinked under a mild condition and the solvent extraction is a critical process to produce mesoporous structure. In the next step, H_2SO_4 was used as material of acidification through ion exchange progress

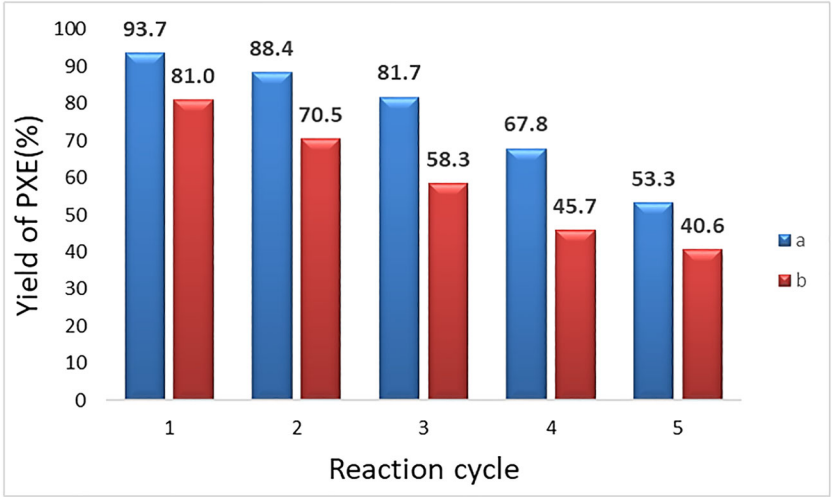

FIGURE 6 The recycling of catalyst a) P (BVS-SO3H)-SO3CF3 and b) P (BVS-SO3H)

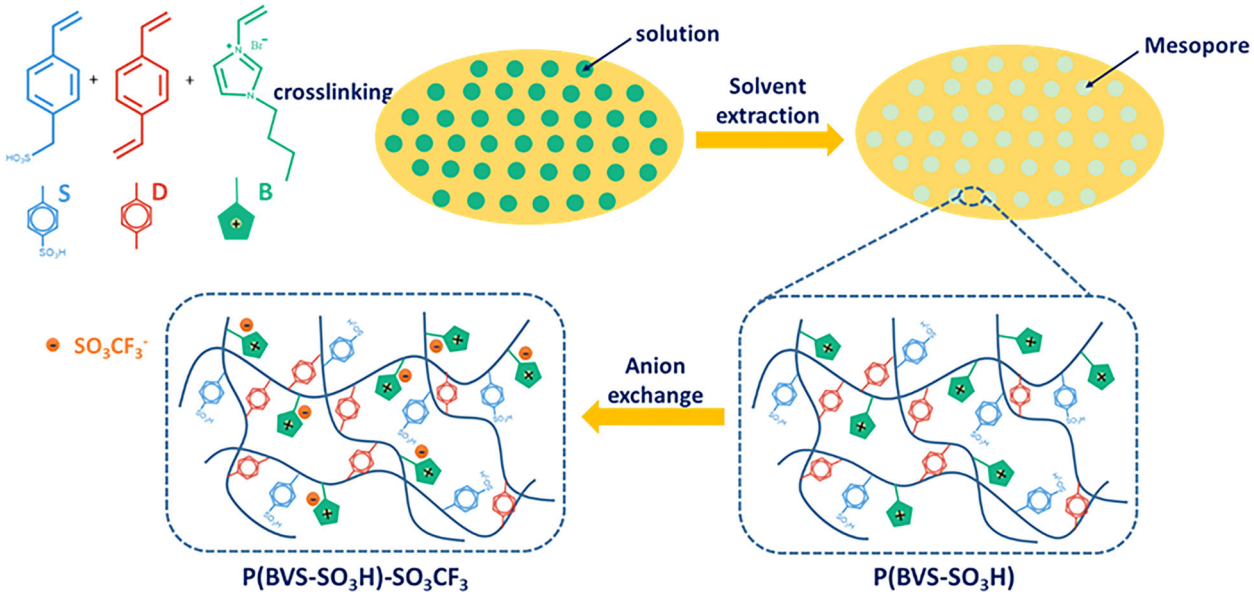

FIGURE 7 Assumptive formation mechanism of ternary dual acidic MILs

to produce P (BVS-SO_3H). The final product P (BVS-SO_3H)-SO_3CF_3 was prepared by anion exchange. And the original network was still keeping stable after functionalization. The morphology difference of P (BVS-SO_3H)-SO_3CF_3 and P (BVS-SO_3Na) may be attributed to the re-crosslinking of polymer during the anion exchange of -SO_3CF_3 which also lead to the reduce of some mesopores inside the product. While the acidic of the sample exhibit a great increase after the introduction of -SO_3CF_3 through the catalyst reaction.

4 | CONCLUSION

In conclusion, a fresh cross-linked mesoporous dual Brønsted acidic poly (ionic liquids) with three monomers was successfully synthesized. Accordingly, dual Brønsted acid-functionalized P (BVS-SO_3H)-SO_3CF_3 was obtained by sulfonating in the polymer framework. And the results proved that the P (BVS-SO_3H)-SO_3CF_3 under the condition of the molar ratio is B:V: S = 1:2:2, the reaction temperature is 120 °C and the addition of catalyst is 0.5 wt% of the reaction system, P (BVS-SO_3H)-SO_3CF_3 catalyst the can achieve the best conversion ratio(100%) and PXE Yield(93.7%) Also, the catalyst contains abundant mesopores and presents great thermal stability and surface area. Comparing to other single acidic solid catalysts, the introduction of -SO_3H and -SO_3CF_3 groups would markedly increase the exposed active acidic sites and finally improved the catalytic performance. As a heterogeneous catalyst, P (BVS-SO_3H)-SO_3CF_3 can be easily detached from the reaction solvent and reduce the cost of the catalyst especially. Furthermore, from a viewpoint of application potential, the sample showed promising catalytic performance in alkylation of o-xylene and styrene. Through this study, it may be possible to develop some novel green Brønsted-based catalyst and time-saving routes for reactions such as Friedel-Crafts reaction, transesterification, esterification, cellulose hydrolysis reaction and so on. This may finally greatly expand the application of solid acidic catalytic materials.

ACKNOWLEDGEMENTS

The authors are grateful to the financial supports of the National Natural Science Foundation of China (Grant No. 21676056, 21376051, 51673040, and 21306023), "Six Talents Pinnacle Program" of Jiangsu Province of China (JNHB-006), Qing Lan Project of Jiangsu Province (1107040167), Fund Project for Transformation of Scientific and Technological Achievements of Jiangsu Province of China (Grant No. BA2014100).

CONFLICT OF INTEREST

There are no conflicts to declare.

ORCID

Xiao Sha https://orcid.org/0000-0002-7377-2293

REFERENCES

[1] V. Malshe, E. Sujatha, *React. Funct. Polym.* **2000**, *43*, 183.

[2] Z. Zhao, Z. Li, G. Wang, W. Qiao, L. Cheng, *Appl. Catal., A* **2004**, *262*, 69.

[3] J. Li, Y. Zhou, M. Dan, G. Chen, X. Wang, X. Yang, M. Wang, M. Peng, J. Wang, *Chem. Eng. J.* **2014**, *254*, 54.

[4] X. Sheng, Y. Zhou, Y. Zhang, Y. Duan, Z. Zhang, Y. Yang, *Microporous Mesoporous Mater.* **2012**, *161*, 25.

[5] R. Noble, D. Gin, *J. Membr. Sci.* **2011**, *369*, 1.

[6] G. Bureros, A. Tanjay, D. Cuizon, A. Go, L. Cabatingan, R. Agapay, Y. Ju, *Renewable Energy* **2019**, *138*, 489.

[7] Y. Zhang, T. Chen, G. Zhang, G. Wang, H. Zhang, *Appl. Catal., A* **2019**, *575*, 38.

[8] X. Zhang, D. Mao, Y. Leng, Y. Zhou, J. Wang, *Catal. Lett.* **2012**, *143*, 193.

[9] Q. Li, B. Wang, Y. Zhang, C. Li, G. Gao, *Chem. Commun.* **2017**, *53*, 3785.

[10] D. I. Mori, R. Martin, R. Noble, D. Gin, *Polymer* **2017**, *112*, 435.

[11] D. Lu, J. Zhao, L. Yan, P. Jiang, C. Zhang, *Catal. Commun.* **2016**, *83*, 27.

[12] W. Qian, T. John, F. Yan, *Chem. Soc. Rev.* **2017**, *46*, 1124.

[13] C. Zhang, W. Zhang, H. Gao, Y. Bai, Y. Sun, Y. Chen, *J. Membr. Sci.* **2017**, *528*, 72.

[14] V. Bui-Thi-Tuyet, G. Trippé-Allard, J. Ghilane, H. Randriamahazaka, *ACS Appl. Mater. Interfaces* **2016**, *8*, 28316.

[15] Y. Feng, L. Li, X. Wang, J. Yang, T. Qiu, *Energy Convers. Manage.* **2017**, *153*, 649.

[16] M. Dule, M. Biswas, T. Paira, T. Mandal, *Polymer* **2015**, *77*, 32.

[17] S. Zhang, D. Kaoru, W. Masayoshi, *Chem. Sci.* **2015**, *6*, 3684.

[18] D. Kuzmicz, P. Coupillaud, Y. Men, V. Joan, V. Giordano, A. Martina, T. Daniel, J. Yuan, *Polymer* **2014**, *55*, 3423.

[19] F. Liu, X. Meng, Y. Zhang, L. Ren, F. Nawaz, F. Xiao, *J. Catal.* **2010**, *271*, 52.

[20] Y. Liu, K. Wang, W. Hou, W. Shan, J. Li, Y. Zhou, J. Wang, *Appl. Surf. Sci.* **2018**, 427, 575.

[21] D. Tao, F. Liu, L. Wang, L. Jiang, *Appl. Catal., A* **2018**, *564*, 56.

[22] W. Zheng, C. Huang, W. Sun, L. Zhao, *J Phys Chem B* **2018**, *122*, 1460.

[23] D. Li, J. Li, D. Mao, H. Wen, Y. Zhou, J. Wang, *Mater. Chem. Phys.* **2017**, *189*, 118.

[24] A. Kausar, *Polym.-Plast. Technol. Eng.* **2017**, *56*, 1823.

[25] X. Suo, L. Xia, Q. Yang, Z. Zhang, Z. Bao, Q. Ren, *J. Mater. Chem. A* **2017**, *5*, 14114.

[26] H. Gao, Y. Zhou, X. Sheng, S. Zhao, C. Zhang, J. Fang, B. Wang, *Appl. Catal., A* **2018**, *552*, 138.

[27] F. Liu, W. Kong, C. Qi, L. Zhu, F. Xiao, *ACS Catal.* **2012**, *2*, 565.

[28] D. Li, D. Mao, J. Li, Y. Zhou, J. Wang, *Appl. Catal., A* **2015**, *510*, 125.

[29] Z. Xu, G. Zhao, U. Latif, M. Wang, A. Wang, Y. Zhang, S. Zhang, *RSC Adv.* **2018**, *8*, 10009.

[30] S. Li, R. Gao, W. Zhang, Y. Zhang, J. Zhao, *Fuel* **2018**, *221*, 1.

[31] D. Li, J. Li, D. Mao, H. Wen, Y. Zhou, J. Wang, *ACS Appl. Mater. Interfaces* **2017**, *9*, 38919.

[32] S. Wen, R.-M. G. Lia, W. Zhang, Y. Zhang, J. Zhao, *Appl. Catal., B* **2017**, *221*, 574.

[33] X. Liang, Y. Zhou, Y. Qu, Y. Han, X. Wang, C. Cheng, A. Duan, L. Zhao, *RSC Adv.* **2018**, *8*, 13750.

[34] F. Yu, Y. Gu, X. Gao, Q. Liu, C. Xie, S. Yu, *Chem Commun.* **2019**, *55*, 4833.

[35] K. Alam, J. Kim, D. Kang, J. Park, *Adv. Synth. Catal.* **2019**, *361*, 1683.

[36] A. Bollu, N. Sharma, *J Org Chem* **2019**, *84*, 5596.

[37] Y. Ouyang, X. Xu, F. Qing, *Angew Chem Int Ed Engl* **2018**, *57*, 6926.

[38] M. Glodek, A. Makal, D. Plazuk, *J Org Chem* **2018**, *83*, 14165.

SUPPORTING INFORMATION

Additional supporting information may be found online in the Supporting Information section at the end of the article.

How to cite this article: Sha X, Sheng X, Zhou Y, Wang B, Liu Y, Bao J. High Catalytic Performance of Mesoporous Dual Brønsted Acidic Ternary Poly (Ionic Liquids) for Friedel-Crafts Alkylation. *Appl Organometal Chem*. 2019;. https://doi.org/10.1002/aoc.5180